Effect of polymer nonideality in a colloid-polymer mixture

P. B. Warren
Unilever Research Port Sunlight Laboratory, Quarry Road East, Bebington, Wirral L63 3JW, United Kingdom

S. M. Ilett and W. C. K. Poon
Department of Physics and Astronomy, The University of Edinburgh, Mayfield Road, Edinburgh EH9 3JZ, United Kingdom
(Received 15 March 1995)

We present a theory for the effect of polymer nonideality on the phase behavior of a hard-sphere colloid plus nonadsorbing polymer mixture. Starting from the behavior at the θ temperature, which has been treated previously within a mean-field framework [H. N. W. Lekkerkerker *et al.*, Europhys. Lett. **20**, 559 (1992)], we use perturbation theory to take into the account the polymer-polymer interaction up to the second virial level. Theoretical predictions of the phase behavior are compared with data obtained in one particular model system: sterically stabilized polymethylmethacrylate particles and random-coil polystyrene dispersed in cis-decahydronaphthalene. Within the same theoretical framework the potential of mean force is calculated between a pair of plates immersed in a nonideal polymer solution. The result, showing a potential barrier in front of an attractive depletion well, is in agreement with a recent calculation by Walz and Sharma [J. Y. Walz and A. Sharma, J. Colloid Interface Sci. **168**, 485 (1994)].

PACS number(s): 82.70.Dd, 64.70.−p, 64.75.+g

I. INTRODUCTION

The phase behavior of colloid-polymer mixtures has attracted attention for many decades (see, e.g., references in [1]). The addition of enough nonadsorbing polymer to an otherwise stable colloidal suspension causes phase separation. The earliest model for this process, which has remained popular since it was suggested 30 years ago, was due to Asakura and Oosawa [2]. In the Asakura-Oosawa (AO) model, the colloids interact as *hard spheres* of radius a. The polymers are assumed to be *freely interpenetrable coils*. The center of a polymer coil is, however, excluded from coming closer than a distance δ from the surface a hard sphere (colloid), where δ, in reality, would be something like the radius of gyration of a polymer molecule. Each hard sphere is therefore surrounded by a "depletion zone" of thickness δ. The only effect of the colloid on the polymer is to restrict the volume in which the latter can move: the *free volume*; see Fig. 1. The overlap of the depletion zones from neighboring colloids increases the total free volume and thus the entropy of the polymers. At high concentrations of either components, this effect leads to phase separation.

The AO model has been used in an "effective potential" treatment of the colloid-polymer problem [3]. The increase in entropy due to overlapping depletion zones of neighboring particles can be seen as inducing an attraction between the particles. Thus the effect of the added polymer can be modeled by an effective potential, the depletion potential $U_{\rm dep}$ [4,5]. The phase behavior of the polymer-free colloid is assumed known. $U_{\rm dep}$ is then used in thermodynamic perturbation theory to calculate the modified phase behavior.

Lekkerkerker *et al.* [6] recently solved the "primitive" version of the AO model in the mean-field approximation. In this primitive approach, the polymer translational degrees of freedom are *not* integrated out to give an effective potential. Instead, the colloid and polymer degrees of freedom are treated on a more equal footing. The free energy of the whole *mixture* is minimized. The topology of the resultant phase diagrams depends sensitively on the ratio of the size of the polymer to that of the colloid, which is given by

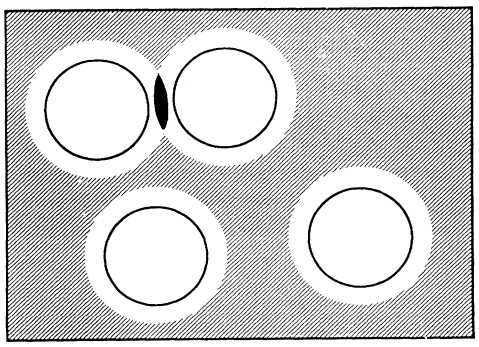

FIG. 1. Schematic illustration of depletion and free volume. Each particle is surrounded by a *depletion zone* (white), the region immediately next to each particle surface, which is inaccessible to the centers of polymer coils. The hatched area is the *free volume* $V_{\rm free}$, which is available to the centers of polymer coils. The overlap of depletion zones (black) gives rise to extra free volume for the polymers and therefore a larger negative contribution to the entropic term of the free energy. This mechanism induces an effective attraction between the particles.

$$\xi = \delta/a \tag{1}$$

in the model. For $\xi \leq 0.32 = \xi_{CO}$ (the crossover size ratio), the only effect of the polymer is to expand the region of coexisting colloidal crystal and fluid phases, which occurs at $0.494 < \phi < 0.545$ for a pure hard-sphere colloid (where ϕ is the colloid volume fraction). At larger size ratios, however, colloidal liquid-gas coexistence becomes possible and a critical point appears on the phase diagram.

These predictions have been tested extensively in one particular model system: monodisperse polymethylmethacrylate (PMMA) particles sterically stabilised by chemically grafted poly-12-hydroxystearic acid and random-coil polystyrene dispersed in cis-decahydronaphthalene (cis-decalin) [7–10]. These experiments, together with similar results reported recently by Leal Calderon *et al.* [11], confirm the broad picture predicted by theory, e.g., the sensitive dependence of phase diagram topology on the polymer-colloid size ratio. However, significant quantitative differences between theory and experiment remain. Reasons for expecting such discrepancies have been discussed in detailed before [7,10], one of which is the very simple model used for the polymer. In the AO model a polymer molecule is supposed to interact with a colloidal particle as a rigid hard sphere. In reality the polymer coil is deformable. The recent computer simulations of Meijer and Frenkel [12] has addressed this issue. In their work, colloidal particles are again hard spheres; the polymer molecules are, however, represented by a simple *lattice* model. In this way, both the nonpairwise additivity of the polymer-induced interaction and the deformability of the polymer molecules are taken into account. (Nonpairwise additivity is also included in the theory of Lekkerkerker *et al.*) Meijer and Frenkel found that, indeed, nonspherical conformations make significant contributions to the free energy, especially at high colloid volume fractions or for long polymers, thus modifying the phase behavior.

In the Meijer-Frenkel simulation, however, the polymer is still treated as *ideal.* That is to say, polymer-polymer interactions are *not* included. In this paper we present an extension of the statistical mechanical treatment of Lekkerkerker *et al.* in order to take into account polymer nonideality up to the second virial level. The model developed is then used to predict the positions of phase boundaries for the colloidal PMMA plus random-coil polystyrene system for two molecular weights $M = 0.39 \times 10^6$ and $M = 2.85 \times 10^6$, at a range of temperatures starting from the theta temperature $T_\theta = 12\,^\circ\mathrm{C}$. The predictions are compared with experimental observations. Data for the case of $M = 0.39 \times 10^6$ have been presented before [7], while data for the larger polymer have not been presented until now. We also use the same model to calculate the potential of mean force between a pair of plates and compare our result with a recent calculation of Walz and Sharma [13]. Finally, in the Appendix, we use the key result of our theory to evaluate the accuracy of an *ad hoc* free energy expression used in the literature recently to treat the phase behavior of hard-sphere mixtures.

II. STATISTICAL MECHANICS

The model statistical mechanical system is as follows. There are N_C colloidal particles and N_P polymer coils in a volume V. The colloidal particles are taken as hard spheres of radius a. That is to say, the colloid-colloid pair interaction $U_{CC}(r)$ is given by

$$U_{CC}(r) = \begin{cases} 0 & (r > 2a) \\ \infty & (r \leq 2a). \end{cases} \tag{2}$$

Insofar as their interaction with colloidal particles are concerned, each polymer coil behaves as a hard sphere of radius δ. In other words, each colloidal particle excludes polymer from a sphere of radius $a + \delta$ around its center. Thus the colloid-polymer pair interaction $U_{CP}(r)$ is given by

$$U_{CP}(r) = \begin{cases} 0 & (r > a + \delta) \\ \infty & (r \leq a + \delta). \end{cases} \tag{3}$$

Finally, the polymer-polymer interaction is modeled by a pair interaction $U_{PP}(r)$, which is assumed to be short range. It turns out that its effect on phase behavior will be measured by the usual second virial coefficient of the polymer B_2.

Denote the colloid positions individually by $\vec{r}_i$ ($i = 1, \ldots, N_C$) and collectively by $\vec{r}_C$. Similarly the individual and collective polymer coordinates are denoted by $\vec{r}_\mu$ and $\vec{r}_P$. The canonical partition function for the colloid-polymer mixture is given by

$$Z = Z_C^{(id)} Z_P^{(id)} \int \frac{d^3\vec{r}_C}{V^{N_C}} e^{-U_{CC}/k_BT} \times \left\{ \int \frac{d^3\vec{r}_P}{V^{N_P}} e^{-U_{CP}/k_BT} e^{-U_{PP}/k_BT} \right\}, \tag{4}$$

where U_{CC} stands for the total colloid-colloid pair interactions $\sum_{i>j} U_{CC}(\vec{r}_i - \vec{r}_j)$. U_{CP} and U_{PP} have similar meanings. The $Z^{(id)}$'s are the ideal partition functions in the absence of interactions:

$$Z_{id}^C = \frac{1}{N_C!} \left(\frac{V}{\lambda_C^3} \right)^{N_C}, \tag{5}$$

$$Z_{id}^P = \frac{1}{N_P!} \left(\frac{V}{\lambda_P^3} \right)^{N_P}, \tag{6}$$

where λ_C and λ_P are the de Broglie thermal wavelengths of the colloid and polymer, respectively.

In outline, the idea of our treatment is as follows. First, the $\exp(-U_{PP}/k_BT)$ in Eq. (4) is expanded in terms of Mayer f functions. Once this is done, the factor $\{\}$ in that equation can be evaluated exactly in the form of a power series in f functions. A weighted sum of the resultant expression for Z over values of N_P may then be performed to convert it to a semigrand partition function Ξ. This gives an effective many-body depletion potential for the colloid particles whose magnitude is controlled by the polymer activity. This depletion potential is then handled by a mean-field–van der Waals approximation. Note that if $U_{PP} = 0$ then this approach corresponds

exactly to that already developed by Lekkerkerker *et al.* [6].

A. Semigrand canonical formalism

To account for the colloid-polymer interaction given by Eq. (3) we introduce a void function $\varphi(\vec{r}_\mu;\vec{r}_C)$

$$\varphi(\vec{r}_\mu;\vec{r}_C)=\prod_i \theta(|\vec{r}_\mu-\vec{r}_i|-(a+\delta)), \tag{7}$$

where $\theta(x)$ is a step function: $\theta(x)=0$ for $x<0$ and $\theta(x)=1$ for $x>0$. Hence the void function in Eq. (7) is zero if the polymer coordinate $\vec{r}_\mu$ lies inside any of the excluded volume spheres of radius $a+\delta$ centered on each colloid and unity if $\vec{r}_\mu$ lies in the free volume (or "void") V_{free}, see Fig. 1:

$$\varphi(\vec{r}_\mu;\vec{r}_C)=\begin{cases}1 & \text{if } \vec{r}_\mu\in V_{\text{free}}\\ 0 & \text{otherwise.}\end{cases} \tag{8}$$

Note that φ is a function of the complete set of colloid coordinates $\vec{r}_C$, which should be considered fixed at this stage. The void function also gives an expression for the exact *free volume fraction*, which we define here for later use:

$$\alpha(\vec{r}_C)=\frac{1}{V}\int \varphi(\vec{r};\vec{r}_C)d^3\vec{r}. \tag{9}$$

In terms of these void functions, the Boltzmann factor of the total colloid-polymer interaction is given by

$$e^{-U_{CP}/k_BT}=\prod_\mu \varphi(\vec{r}_\mu;\vec{r}_C). \tag{10}$$

To deal with the polymer-polymer interaction, we introduce the Mayer f function

$$f_{\mu\nu}=f(|\vec{r}_\mu-\vec{r}_\nu|)=1-e^{-U_{PP}(|\vec{r}_\mu-\vec{r}_\nu|)/k_BT}. \tag{11}$$

(Note that this f is the negative of that usually defined.) $f_{\mu\nu}$ is small and nonzero only for $|\vec{r}_\mu-\vec{r}_\nu|\approx\delta$ or smaller. The total polymer-polymer Boltzmann factor appearing in Eq. (4) can be written as a product

$$e^{-U_{PP}/k_BT}=\prod_{\mu>\nu}[1-f_{\mu\nu}]. \tag{12}$$

Our perturbative approach is in terms of the Mayer functions, just as in the theory of ordinary, imperfect gases [14]. Thus we write

$$e^{-U_{PP}/k_BT}=1-\sum_{\mu>\nu} f_{\mu\nu}+O(f^2). \tag{13}$$

Using Eqs. (7), (10), and (13), we can now integrate over the polymer degrees of freedom in Eq. (4). This yields

$$Z=Z_C^{(id)}Z_P^{(id)}\int\frac{d^3\vec{r}_C}{V^{N_C}}e^{-U_{CC}/k_BT}\times\left\{[\alpha(\vec{r}_C)]^{N_P}-[\alpha(\vec{r}_C)]^{N_P-2}\frac{N_P(N_P-1)}{2}\times\int\frac{d^3\vec{r}_1d^3\vec{r}_2}{V^2}f_{12}\varphi(\vec{r}_1;\vec{r}_C)\varphi(\vec{r}_2;\vec{r}_C)+O(f^2)\right\}, \tag{14}$$

where we have used the definition of the exact free volume fraction introduced in Eq. (9).

Now form the semigrand partition function Ξ by introducing the polymer chemical potential μ_P

$$\Xi=\sum_{N_P=0}^{\infty}e^{N_P\mu_P/k_BT}Z(N_P). \tag{15}$$

The physical picture motivating this approach is that of a reservoir of pure polymer solution in osmotic equilibrium with the colloid-polymer mixture [15].

The two terms in Eq. (14) give rise to two terms in Ξ

$$\Xi=\Xi_1-\Xi_2. \tag{16}$$

Defining the integral operator

$$Z_C\equiv Z_C^{(id)}\int\frac{d^3\vec{r}_C}{V^{N_C}}e^{-U_{CC}/k_BT}, \tag{17}$$

we find that the first term in Eq. (16) is

$$Z_C\sum_{N_P=0}^{\infty}\frac{1}{N_P!}\left(\frac{V}{\lambda_P^3}\right)^{N_P}[\alpha(\vec{r}_C)]^{N_P}\exp[\mu_PN_P/k_BT],$$

which sums to

$$\Xi_1=Z_C\exp[(V/\lambda_P^3)\alpha(\vec{r}_C)e^{\mu_P/k_BT}]. \tag{18}$$

Similarly the second term in Eq. (16) is

$$Z_C\sum_{N_P=2}^{\infty}\frac{1}{N_P!}\left(\frac{V}{\lambda_P^3}\right)^{N_P-2}\exp[\mu_PN_P/k_BT]\times\frac{N_P(N_P-1)}{2}\int\frac{d^3\vec{r}_1d^3\vec{r}_2}{V^2}f_{12}\varphi_1\varphi_2,$$

where we have introduced the obvious abbreviations

$$\varphi(\vec{r}_\mu;\vec{r}_C)=\varphi_\mu. \tag{19}$$

This second term sums to

$$\Xi_2=\frac{Z_C}{2}\left(\frac{V}{\lambda_P^3}\right)^2e^{2\mu_P/k_BT}\exp[(V/\lambda_P^3)\alpha(\vec{r}_C)e^{\mu_P/k_BT}]\times\int\frac{d^3\vec{r}_1d^3\vec{r}_2}{V^2}f_{12}\varphi_1\varphi_2. \tag{20}$$

Introducing the polymer activity

$$a_P=\frac{e^{\mu_P/k_BT}}{\lambda_P^3}, \tag{21}$$

we find that the two terms in Ξ now combine to the simple form

$$\Xi = Z_C \exp[V\alpha(\vec{r}_C)a_P]\left(1 - \frac{1}{2}a_P^2 \int d^3\vec{r}_1 d^3\vec{r}_2 f_{12}\varphi_1\varphi_2\right). \tag{22}$$

Noting that $1-x = e^{-x}$ to first order in x and substituting back the integral operator for Z_C from Eq. (17) we get finally

$$\Xi = Z_C^{id} \int \frac{d^3\vec{r}_C}{V^{N_C}} \exp[-U_{CC}/k_BT + a_P\alpha(\vec{r}_C)V - \frac{1}{2}a_P^2 \int d^3\vec{r}_1 d^3\vec{r}_2 f_{12}\varphi(\vec{r}_1;\vec{r}_C)\varphi(\vec{r}_2;\vec{r}_C) + O(f^2)]. \tag{23}$$

This equation is *exact* to first order in the Mayer function f.

B. Mean-field–van der Waals approximation

To proceed further we make the mean-field–van der Waals approximation, which consists of replacing the $\{\vec{r}_C\}$-dependent terms in the exponential in Eq. (23) by their *averages* over the *unperturbed* colloid (hard-sphere) system

$$\alpha(\vec{r}_C) \to \langle\alpha(\vec{r}_C)\rangle_0 = \alpha(\phi), \tag{24}$$

$$\varphi_1\varphi_2 \to \langle\varphi_1\varphi_2\rangle_0 = g_{vv}(|\vec{r}_1 - \vec{r}_2|, \phi). \tag{25}$$

In these equations, the subsript in $\langle\,\rangle_0$ denotes preaveraging over the *unperturbed* colloid configurations. We have introduced the average free volume fraction $\alpha(\phi)$ and the void-void correlation function $g_{vv}(|\vec{r}_1 - \vec{r}_2|, \phi)$, both of which are now functions of the colloid volume fraction ϕ. Note that $\varphi_1\varphi_2$ takes the value unity only if both $\vec{r}_1$ and $\vec{r}_2$ are in the free volume; otherwise $\varphi_1\varphi_2 = 0$.

The semigrand potential Ω, related to the semigrand canonical partition function by

$$\Omega = -k_BT \ln \Xi, \tag{26}$$

is therefore given by

$$\Omega = F_C - Vk_BTa_P\alpha + \frac{1}{2}Vk_BTa_P^2 \int d^3\vec{r} f(r) g_{vv}(r) + O(f^2), \tag{27}$$

where $F_C = -k_BT \ln Z_C$ is the Helmoltz free energy of the (unperturbed) colloid. In Eq. (27), F_C, α, and $g_{vv}(r)$ are all functions of the colloid volume fraction ϕ. $F_C(\phi)$ is, of course, well approximated by either the Carnahan-Starling equation of state [16] in the fluid state or the parametric fit of Hall [17] in the solid state.

Equation (27) is the key result of this paper. To proceed further and calculate phase behavior using this result, we need to know something about the average free volume fraction α and the void-void correlation function $g_{vv}(r)$.

C. Free volume fraction and void correlation

A closed-form expression for the average free volume fraction as a function of the colloid volume fraction $\alpha(\phi)$ can be obtained through scaled particle theory results for hard-sphere mixtures (see references and explanation in [6] and [15]):

$$\alpha = (1-\phi)\exp[-A\gamma - B\gamma^2 - C\gamma^3], \tag{28}$$

in which $\gamma = \phi/(1-\phi)$, $A = 3\xi+3\xi^2+\xi^3$, $B = 9\xi^2/2+3\xi^3$, and $C = 3\xi^3$ ($\xi = \delta/a$ is the size ratio). Meijer and Frenkel [12] have shown recently by computer simulation that this expression is reasonably accurate even for dense fluid and crystalline phases.

A corresponding expression for the void-void correlation function is not available. Its value in two limits is, however, obtainable trivially. First, as $r \to \infty$ we expect the two void functions to be decoupled, so that

$$\langle\varphi(\vec{r}_1;\vec{r}_C)\varphi(\vec{r}_2;\vec{r}_C)\rangle_0 \to \langle\varphi(\vec{r}_1;\vec{r}_C)\rangle_0\langle\varphi(\vec{r}_2;\vec{r}_C)\rangle_0 = \alpha^2, \tag{29}$$

i.e., $g_{vv}(r) \to \alpha^2$ as $r = |\vec{r}_1 - \vec{r}_2| \to \infty$. Second, as $r \to 0$, the two void functions making up the correlation function are either both zero or both unity, i.e., $\varphi^2 = \varphi$, so that

$$\langle\varphi(\vec{r}_1;\vec{r}_C)\varphi(\vec{r}_2;\vec{r}_C)\rangle_0 \to \langle[\varphi(\vec{r}_1;\vec{r}_C)]^2\rangle_0 = \langle\varphi(\vec{r}_1;\vec{r}_C)\rangle_0 = \alpha. \tag{30}$$

That is to say, $g_{vv}(r) \to \alpha$ as $r = |\vec{r}_1 - \vec{r}_2| \to 0$.

A summary of the current knowledge on the void-void correlation can be found in the very illuminating review on scaled particle theory and related subjects by Reiss [18]. These results, plus our own simulations [19], suggest that (i) the range over which $g_{vv}(r)$ is expected to decay from α (at $r = 0$) to α^2 is of the order of the colloid radius a and (ii) $g_{vv}(r)$ has finite (negative) slope at $r = 0$. We therefore approximate the void-void correlation function by a simple exponential with the appropriate range and limiting values

$$g_{vv}(r) = \alpha^2 + \alpha(1-\alpha)e^{-r/a}. \tag{31}$$

Equations (28) and (31) are the results we need for use in the semigrand potential Eq. (27).

D. Temperature effect on the polymer

The final step before we can use Eq. (27) to calculate phase behavior is to formulate the semigrand potential in terms of measurable polymer properties. To do so, we first seek to put Eq. (27) in a more suggestive form by noting that the usual second virial coefficient of a polymer is defined in terms of the Mayer function as

$$B_2 = \frac{1}{2}\int d^3\vec{r} f(r). \tag{32}$$

The form of the third term in Eq. (27) then suggests that

we define a *renormalized* second virial coefficient by

$$\tilde{B}_2 = \frac{1}{2}\int d^3\vec{r} f(r)\frac{g_{vv}(r)}{\alpha} = \frac{1}{2}\int d^3\vec{r}[1-e^{-U_{PP}(r)/k_BT}]\frac{g_{vv}(r)}{\alpha}, \quad (33)$$

so that Eq. (27) becomes

$$\Omega = F_C - a_P k_B T(1-a_P\tilde{B}_2)\alpha V. \quad (34)$$

[The reason for including the $1/\alpha$ in the definition of $\tilde{B}_2$, and therefore getting Eq. (34) into the form it takes, is to facilitate comparison with Eq. (A5) in the Appendix.]

We do not have detailed knowledge of the form of the polymer-polymer pair potential $U_{PP}(r)$, except that we expect it to have a range of the order δ. We therefore take a square well potential of height U_0 and range δ for this interaction:

$$U_{PP}(r) = \begin{cases} U_0 & \text{if } r<\delta \\ 0 & \text{otherwise.} \end{cases} \quad (35)$$

Using this form of the polymer-polymer interaction and the model void-void correlation function given in Eq. (31) we find

$$B_2 = \frac{2}{3}\pi\delta^3(1-e^{-U_0/k_BT}), \quad (36)$$

$$\frac{\tilde{B}_2}{B_2} = 1-(1-\alpha)\left[1-6\xi^3+3e^{-\xi}(\xi+2\xi^2+2\xi^3)\right], \quad (37)$$

where $\xi=\delta/a$ is the size ratio previously defined. If we expand the above expression for $\tilde{B}_2$ at small ξ we get

$$\tilde{B}_2 = B_2\left[1-\frac{3}{4}(1-\alpha)\xi+\cdots\right]. \quad (38)$$

All that remains now is to find out how B_2 and the polymer size (and therefore δ and ξ) increase away from the θ temperature. Both processes are ultimately controlled by monomer-monomer interactions, which can be measured by the "Fixman parameter" z [20]. At the theta temperature T_θ, $z=0$ and a polymer coil is at its most ideal. The rate at which z increases from zero, which is a measure of polymer nonideality, is governed both by the molecular weight (M) of the polymer molecule and the temperature (T, in degrees Kelvin). For polystyrene in a whole range of simple hydrocarbon solvents (including cis-decalin), Berry [21] found that

$$z = 0.009\,75\sqrt{M}\left(1-\frac{T_\theta}{T}\right). \quad (39)$$

To first order in z, the radius of gyration r_g is given by [20,21]

$$\frac{r_g^2}{{}^0r_g^2} = 1+\frac{134}{105}z+O(z^2), \quad (40)$$

where ${}^0r_g$ is the radius of gyration at the θ temperature. We assume that our exclusion length parameter δ scales directly as r_g.

The second virial coefficient as a function of z is also known to low order [20,21]

$$\frac{B_2}{4\pi^{3/2}r_g^3} = z-4.8z^2+O(z^3), \quad (41)$$

where we have ignored a slight difference in the scaling of the radius of gyration and the root mean square end to end separation in arriving at this approximate expression. The data of Berry [21] show that the approximations in Eqs. (40) and (41) are accurate to $z\approx 0.1$.

III. EFFECT ON PHASE BEHAVIOR

Equation (34), together with the definition of the renormalized second virial coefficient in Eq. (33) and the information on the polymer given by Eqs. (38)–(41), can now be used to calculate the phase behavior of our model mixture. The procedure, for a polymer of a particular molecular weight and at a particular temperature, is to calculate the Fixman parameter using Eq. (39). The depletion layer thickness is then determined using Eq. (40) and the second virial coefficient is calculated using Eq. (41). These values are then substituted into Eq. (38) to give the renormalized second virial coefficient $\tilde{B}_2$. Equation (34) can now be used to determine phase behavior using standard methods (see, e.g., [6]).

A comparison of our theory with experimental data for colloidal PMMA plus random-coil polystyrene in cis-decalin at two size ratios $\xi\approx 0.08$ and $\xi\approx 0.24$ is presented. Polystyrene in cis-decalin has a θ temperature of $T_\theta = 285$ K. The comparison with theory in each case is limited to that range of temperatures in which the Fixman parameter z, Eq. (39), is less than 0.1, beyond which higher-order terms in Eqs. (40) and (41) need to be taken into account. For the smaller size ratio $\xi\approx 0.08$ (polymer molecular weight $M=0.39\times 10^6$), we can compare experiment with theory over the range 285 K$< T \lesssim$ 290 K. For the larger size ratio $\xi\approx 0.24$ (polymer molecular weight $M=2.85\times 10^6$), however, the requirement of $z\lesssim 0.1$ limits the range of temperature over which our theory is valid to a very small interval 285 K$< T \lesssim$ 287 K.

First, consider the size ratio of $\xi\approx 0.08$. This is achieved experimentally using polystyrene of molecular weight $M=0.39\times 10^6$ and colloidal PMMA of radius $a=218$ nm. At high enough polymer concentrations in this system, phase separation into colloidal crystal and fluid phases is observed; see [7] for details. The effect of temperature on this system has also been investigated previously. The amount of polymer needed for phase separation to occur at the fixed colloid volume fraction of $\phi=0.2$ is reproduced from [7] in Fig. 2, where the prediction of our perturbation theory using $\delta=17.6$ nm (at T_θ) is also plotted. (${}^0r_g$ for this molecular weight, according to Berry [21], should be 17.5 nm.) The agreement is seen to be very satisfactory.

At higher polymer concentrations in this system, equilibrium phase separation into colloidal fluid and crystal

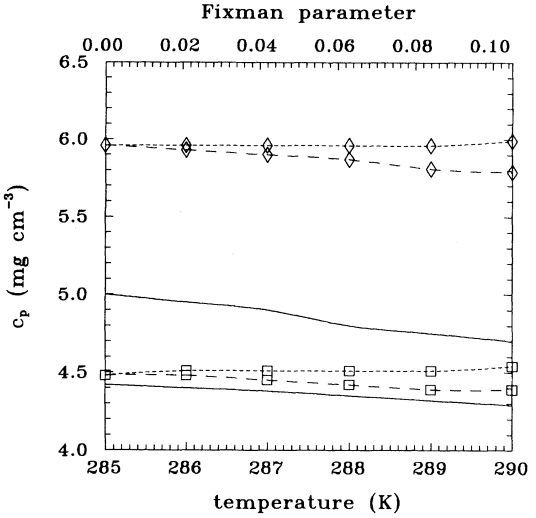

FIG. 2. Comparison between theory and experiment for the size ratio of $\xi = 0.08$. The colloid volume fraction is $\phi = 0.2$. The vertical axis gives polymer concentration in mg/cm^3. The lower horizontal axis gives the temperature, starting from $T_\theta = 285$ K. The upper horizontal axis indicates the corresponding values of the Fixman parameter z. Note that our perturbation theory applies only up to $z \approx 0.1$. Continuous lines are experimental phase boundaries taken from [7]. Below the lower line, the single-phase fluid is stable. Between the two continuous lines, samples separate into coexisiting colloidal fluid and crystal phases. Above the upper continuous line, crystallization is suppressed and nonequilibrium states are observed. The dashed (lower) and dotted (upper) lines through the squares (□) are predictions of our theory for the fluid-crystal phase boundary with and without taking into account coil swelling. The dashed (lower) and dotted (upper) lines through the diamonds (◇) are predictions of our theory for the metastable gas-liquid boundary, again with and without taking into account coil swelling.

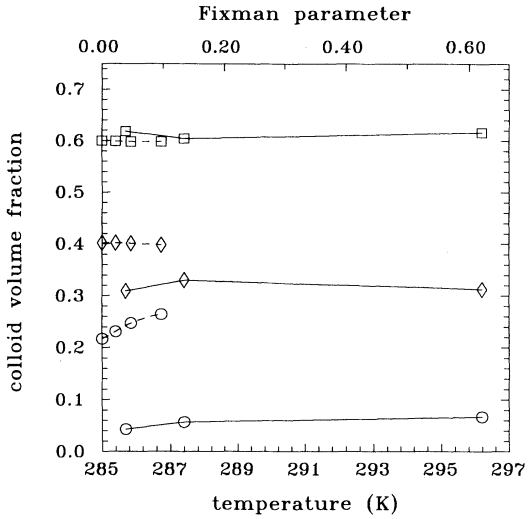

FIG. 3. Colloid concentrations of coexisting gas, liquid, and solid phases predicted by our theory at the theoretical crossover size ratio $\xi = 0.33$ are plotted against temperature and the Fixman parameter z as dashed curves: ○, = gas; ◇, liquid; and □, solid. Note that our perturbation theory is expected to apply only up to $z \approx 0.1$. The experimental data described in Table I are also plotted as continuous lines: ○, gas; ◇, liquid; and □, solid. Within experimental errors (see Table I), the observed volume fractions of the colloidal solid and liquid phases remain constant. The observed increase in volume fraction of the colloidal gas phase with temperature is, however, larger than experimental errors and is a real effect.

is suppressed. Instead, a variety of nonequilibrium behavior is observed, cumulating in a "transient gel" state at the highest polymer concentrations [7,22,23]. It has been suggested [1,23] that the abrupt onset of nonequilibrium behavior in this system is related to the metastable liquid-gas phase boundary hidden within the fluid-crystal two-phase region in the equilibrium phase diagram. (Invoking such "metastable phase boundaries" within equilibrium two-phase regions as an explanation of unexpected, nonequilibrium behavior is a well known and successful practice in metallurgy. See De Hoff's discussion in [24].) The positions of the metastable liquid-gas phase boundary at $\phi = 0.2$ at various temperatures predicted by our model are also plotted in Fig. 2. It is seen that the *slope* of this curve agrees well with that of the experimental gel boundary, even though the absolute position is too high by approximately 20%. This provides support for the speculation in [1].

Note that it is crucial to take into account the *twin* effects of increasing monomer-monomer interactions: increasing osmotic pressure and coil swelling. The predictions of our perturbative treatment *without* taking into account coil swelling are also shown in Fig. 2; the results are not satisfactory in this case.

Experimentally, the phase diagram topology switches at a size ratio of $\xi \approx 0.24$, with polystyrene of molecular weight $M = 2.85 \times 10^6$ [10]. At this size ratio, a stable colloidal liquid phase becomes possible. Therefore, three-phase coexistence between colloidal gas, liquid, and solid phases can be observed. We have measured the colloid concentrations of these coexisting phases as functions of temperature (using methods detailed in [10]) and the results are given in Table I, and are plotted as func-

TABLE I. Dependence of three-phase coexistence compositions on temperature.

Temperature (K)	ϕ_{gas}	ϕ_{liq}	ϕ_{solid}
285	0.043 ± 0.004	0.31 ± 0.05	0.618 ± 0.006
287	0.057 ± 0.004	0.33 ± 0.01	0.612 ± 0.006
296	0.067 ± 0.004	0.312 ± 0.004	0.616 ± 0.006

tions of both the temperature and the Fixman parameter, Eq. (39), in Fig. 3.

The theory of Lekkerkerker *et al.* [6] predicts that the crossover in phase diagram topology occurs at $\xi \approx 0.33$. Here we show the calculated colloid concentrations for coexisting gas, liquid, and solid phases with $\xi = 0.33$ (at T_θ) as functions of the temperature and the Fixman parameter in Fig. 3. Note that the approximations used in our theory become increasingly invalid at $z \approx 0.1$ or above. With this proviso, however, the comparison between theory and experiment is again seen to be reasonable. The initial effect of the temperature rising above T_θ is predicted to be primarily a rise in ϕ_{gas}, with ϕ_{cryst} and ϕ_{liquid} remaining more or less constant. This is confirmed by the data shown in Table I, although the rise in ϕ_{gas} is not as rapid as that predicted by theory.

IV. POTENTIAL OF MEAN FORCE

Finally, within the theoretical framework presented in Sec. II, we can derive an expression for the interaction potential between a pair of flat plates immersed in a mixture of colloids and polymers. It turns out that the effect of polymer nonideality is to induce a repulsive barrier in front of the attractive depletion well. Our final result gives satisfactory agreement with a recent calculation of Walz and Sharma [13], who treated the same phenomena within a different theoretical framework.

We start with the exact expression for the semigrand partition function to first order in the Mayer function: Eq. (23), with Eq. (9) for α. This gives the polymer-induced contribution to the free energy or potential of mean force

$$\Delta F = -a_P k_B T \int \varphi(\vec{r})\, d^3\vec{r} + \frac{1}{2} a_P^2 k_B T \int \varphi(\vec{r}_1)\varphi(\vec{r}_2) f(|\vec{r}_1 - \vec{r}_2|)\, d^3\vec{r}_1\, d^3\vec{r}_2, \tag{42}$$

where $\varphi(\vec{r})$ is the void function appropriate for the geometry under consideration. We introduce the identity $1 = \int_0^\infty \delta(r - |\vec{r}_1 - \vec{r}_2|)\, dr$ to separate out the Mayer function and arrive at

$$\Delta F = -a_P k_B T V_f + \frac{1}{2} a_P^2 k_B T \int_0^\infty f(r)\, S(r)\, dr, \tag{43}$$

where $V_f = \int \varphi(\vec{r})\, d^3\vec{r}$ is the exact free volume and

$$S(r) = \int \varphi(\vec{r}_1)\varphi(\vec{r}_2)\delta(r - |\vec{r}_1 - \vec{r}_2|)\, d^3\vec{r}_1\, d^3\vec{r}_2 \tag{44}$$

is a function that, in a pure suspension, is related to the void-void correlation function by $4\pi r^2 g_{VV}(r) = S(r)/V$. In the finite geometry of a pair of plates, the use of a void-void correlation function is inappropriate.

The key is to give a geometrical interpretation to $S(r)$ that is easily calculable. To do this we define s and $\bar{s}$ by

$$\int \varphi(\vec{r}_2)\delta(r - |\vec{r}_1 - \vec{r}_2|)\, d^3\vec{r}_2 = s(r;\vec{r}_1) = 4\pi r^2 - \bar{s}(r;\vec{r}_1). \tag{45}$$

Clearly s is the *free surface area* of a test sphere of radius r centered at $\vec{r}_1$, i.e., the surface area that does not lie in the excluded volume, and $\bar{s}$ is the surface area that is blocked off by the excluded volume (see Fig. 4). Given these definitions, the function $S(r)$ and a complementary function $\bar{S}(r) = 4\pi r^3 V_f - S(r)$ are calculable as integrals of s and $\bar{s}$, respectively. From Eqs. (44) and (45) we have

$$S(r) = \int \varphi(\vec{r}_1)\, s(r;\vec{r}_1)\, d^3\vec{r}_1 = 4\pi r^2 V_f - \bar{S}(r), \tag{46}$$

$$\bar{S}(r) = \int \varphi(\vec{r}_1)\, \bar{s}(r;\vec{r}_1)\, d^3\vec{r}_1. \tag{47}$$

Inserting these into the expression for the potential of mean force and using $B_2 = \frac{1}{2}\int_0^\infty f(r) 4\pi r^2\, dr$ gives finally

$$\Delta F = -a_P k_B T (1 - a_P B_2) V_f - \frac{1}{2} a_P^2 k_B T \int_0^\infty f(r)\, \bar{S}(r)\, dr. \tag{48}$$

This is now suitable for use in calculations since $\bar{S}$ is a well defined function.

Consider two plates (area A) a distance h apart. On either side of each plate there is a layer of excluded volume (depletion layer) of thickness d (see Fig. 4). The free volume is then given by

$$V_f = \begin{cases} \text{const} + A(2d - h), & 0 < h < 2d \\ \text{const}, & 2d < h. \end{cases} \tag{49}$$

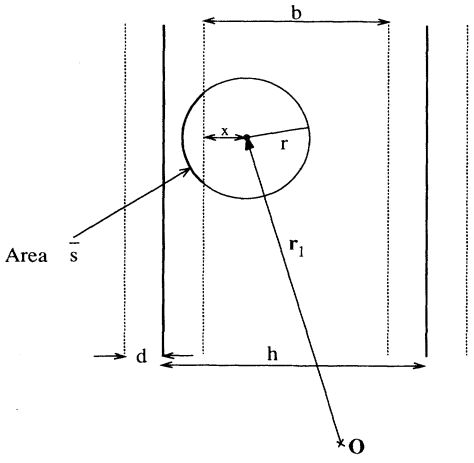

FIG. 4. Geometry used for calculating the potential of mean force. The plates are represented by bold lines. The dotted lines represent depletion layers of thickness d on either side of each plate: these are regions of space inaccessible to polymer molecules. A test sphere centered at position $\vec{r}_1$ of radius r is also shown. The portion of its surface area not contained in the free volume $\bar{s}(r;\vec{r}_1)$ is picked out in bold. The width of the free volume between the two plates is denoted by b and the center of the test sphere is at a distance x from the edge of a depletion layer.

Now consider the blocked-off surface area of a test sphere of radius r at a distance x from the edge of the depletion layer. It is (in three dimensions)

$$\bar{s}(r;x) = \begin{cases} 2\pi r^2(1-x/r), & 0 < x < r \\ 0, & r < x. \end{cases} \tag{50}$$

Thus, in the expression

$$\bar{S}(r) = \int \bar{s}(r;\vec{r}_1)\,\varphi(\vec{r}_1)\,d^3\vec{r}_1, \tag{51}$$

the contribution from an outer surface of a plate is

$$\int_0^r 2\pi r^2(1-x/r)\,A\,dx = \pi r^3 A. \tag{52}$$

This will also be the contribution from an inner surface provided the edges of the depletion layers are at least a distance r apart (i.e., $h > 2d + r$). If this is not the case, the test sphere of radius r cannot completely move away from the edge of the inner depletion layer before its center enters the depletion layer associated with the opposite plate. Denoting the distance between edges of the depletion layers by $b = h - 2d$ for convenience, the contribution to Eq. (51) in this case ($0 < b < r$) is

$$\int_0^b 2\pi r^2(1-x/r)\,A\,dx = 2\pi r^2 A(b - b^2/2r). \tag{53}$$

Combining these we get

$$\bar{S}(r)/A = \begin{cases} 2\pi r^3, & -2d < b < 0 \\ 2\pi r^3 + 4\pi r^2(b - b^2/2r), & 0 < b < r \\ 4\pi r^3, & r < b. \end{cases} \tag{54}$$

Although the calculation could be continued in terms of moments of the Mayer function, it is clearer to introduce a model square potential for which $f(r) = f_0$ for $r < 2d$ and $f(r) = 0$ for $r > 2d$. The interpretation is that the polymer coils act as spheres of radius d, with a constant potential of interaction independent of the degree of mutual overlap. This includes the hard-sphere case $f_0 = 1$. The second virial coefficient is $B_2 = 16\pi d^3 f_0/3$. From Eq. (48), the potential of mean force is

$$\Delta F = -a_P k_B T(1 - a_P B_2)\,V_f - \frac{1}{2}a_P^2 k_B T f_0 \int_0^{2d} \bar{S}(r)\,dr. \tag{55}$$

Dropping the unimportant constant associated with V_f, the integration can be performed to get a piecewise continuous potential

$$\frac{\Delta F}{a_P k_B T A d} = \begin{cases} (1 - a_P B_2)\dfrac{b}{d} - \dfrac{3}{4}a_P B_2, & -2d < b < 0 \\ -\left(\dfrac{3}{4} + \dfrac{b}{d} - \dfrac{3}{8}\dfrac{b^2}{d^2} + \dfrac{1}{64}\dfrac{b^4}{d^4}\right) a_P B_2, & 0 < b < 2d \\ -\dfrac{3}{2}a_P B_2, & 2d < b. \end{cases} \tag{56}$$

These results show that there is a potential barrier in front of the depletion well of range $2d$ and height $\frac{3}{4}a_P^2 k_B T B_2 d$.

The potential in Eq. (56) is identical to the result derived by Walz and Sharma [13], Eq. (24) in their paper, provided that polymer activity is expressed in terms of polymer concentration at infinity (or equivalently polymer reservoir concentration; see the Appendix), and the constant $\frac{3}{2}a_P^2 k_B T B_2 d$ is added to the potential. We note in passing that Clark and Lal observed a repulsive barrier in front of the attractive depletion well in Monte Carlo simulations of nonadsorbing, excluded-volume chains confined between plane walls [27].

An exact calculation is also possible for the excluded-volume shells of a pair of spherical colloid particles, provided they do not overlap. This is because a test sphere intersects the excluded-volume shells in at most two disjoint pieces. When the shells overlap, a complicated three-body overlap problem is encountered.

The origin of the repulsive barrier is clear from the above derivation. In general terms there is a contribution to the free energy from the surface area of the free volume. For polymers in a good solvent this is a negative contribution because pairs of polymers adjacent to the surface of the excluded-volume do not experience the full set of possible mutual configurations that are available in the bulk. Specifically for our example, as the plates are brought together there is a reduction from four surfaces to two surfaces when the inner excluded-volume layers start to overlap. The negative contribution to the free energy becomes less negative, producing a barrier in the potential of mean force. The sharp reduction in surface area is smoothed by the finite range of the polymer-polymer interaction.

V. CONCLUSION

Starting from the behavior of a colloid-polymer mixture at the θ temperature of the polymer [6], we have used perturbation theory to take into the account polymer-polymer interactions up to second virial level. Theoretical predictions of the effects of polymer nonideality on phase behavior are compared with data obtained in mixtures of PMMA colloids and random-coil polystyrene dispersed in cis-decalin. For the limited range of temperatures in which our lowest-order perturbation calculations should be valid, there is satisfactory agreement between theory and experiment. Moreover, the predicted temperature dependence of a metastable liquid-gas binodal in a

mixture with small polymers points to its role in causing the experimentally observed onset of nonequilibrium behavior in such a mixture. Within the same theoretical framework, we have calculated the potential of mean force between a pair of plates immersed in a nonideal polymer solution. The result, showing a potential barrier in front of an attraction depletion well, is in agreement with a recent calculation by Walz and Sharma [13].

ACKNOWLEDGMENTS

We thank Henk Lekkerkerker and Peter Pusey for critical discussions on the subject matter of this manuscript. The work at Edinburgh is partly funded by the United Kingdom Agriculture and Food Research Council (now the Biotechnology and Biological Sciences Research Council).

APPENDIX: COMPARISON WITH RECENT WORK

In two recent papers [25,26], the phase behavior of an asymmetric hard-sphere mixture (spheres of sizes $a_1 > a_2$) has been treated using an approximate expression for the semigrand canonical potential

$$\Omega = F_1(\phi_1) - \Pi_2^{(R)}(\mu_2)\alpha V, \tag{A1}$$

where F_1 is the Helmoltz free energy of a pure system of species 1, $\Pi_2^{(R)}$ is the osmotic pressure of a reservoir of pure species 2 in osmotic equilibrium with the actual mixture, and αV is the free volume available to the center of a single sphere of species 2 in a pure system of 1. Equation (A1) is an approximation. In this appendix, we discuss how good this approximation is in the light of the perturbative treatment of the colloid-polymer problem we have presented in the main body of the paper.

Consider the colloid-polymer semigrand potential in the form given in Eq. (34). Using the relations

$$N_P = \frac{\partial\Omega}{\partial\mu_P} = -\frac{a_P}{k_BT}\frac{\partial\Omega}{\partial a_P}, \tag{A2}$$

$$\Pi_P = -\frac{\partial\Omega}{\partial V} \tag{A3}$$

on Eq. (34) and setting $N_C = 0$, we can calculate the osmotic pressure $\Pi_P^{(R)}$ and number density $n_P^{(R)}$ in a reservoir of pure polymer. Remembering that $\alpha = 1$ and $\tilde{B}_2 = B_2$ when $N_C = 0$, the results are

$$n_p^{(R)} = a_P(1 - 2a_PB_2), \tag{A4}$$

$$\Pi_P^{(R)} = a_Pk_BT(1 - a_PB_2). \tag{A5}$$

Note, before we go on, that on eliminating the polymer activity a_P between these two equations we get back the usual relation

$$\Pi_P^{(R)} = n_P^{(R)}k_BT(1 + n_P^{(R)}B_2). \tag{A6}$$

Now, comparing Eq. (34) with Eq. (A5), we see that the use of $\Pi_P^{(R)}$ Eq. (A1) is tantamount to making $\tilde{B}_2 = B_2$, which, according to Eq. (38), is in error by order $\xi = \delta/a$.

[1] W. C. K. Poon and P. N. Pusey, in *Observation, Prediction and Simulation of Phase Transitions in Complex Fluids*, Vol. 460 of *NATO Advanced Study Institute, Series C: Mathematical and Physical Sciences*, edited by M. Baus, L. R. Rull, and J. P. Ryckaert (Kluwer Academic, Dordrecht, 1995), p. 3.
[2] S. Asakura and F. Oosawa, J. Chem. Phys. **22**, 1255 (1954).
[3] A. P. Gast, C. K. Hall, and W. B. Russel, J. Colloid Interface Sci. **96**, 251 (1983).
[4] S. Asakura and F. Oosawa, J. Polym. Sci. **33**, 183 (1958).
[5] A. Vrij, Pure Appl. Chem. **48**, 471 (1976).
[6] H. N. W. Lekkerkerker, W. C. K. Poon, P. N. Pusey, A. Stroobants, and P. B. Warren, Europhys. Lett. **20**, 559 (1992).
[7] W. C. K. Poon, J. S. Selfe, M. B. Robertson, S. M. Ilett, A. D. Pirie, and P. N. Pusey, J. Phys. (France) II **3**, 1075 (1993).
[8] P. N. Pusey, W. C. K. Poon, S. M. Ilett, and P. Bartlett, J. Phys. Condens. Matter **6**, A29 (1994).
[9] S. M. Ilett, W. C. K. Poon, P. N. Pusey, A. Orrock, M. K. Semmler, and S. Erbil, Prog. Colloid Poly. Sci. **97**, 80 (1994).
[10] S. M. Ilett, A. Orrock, W. C. K. Poon, and P. N. Pusey, Phys. Rev. E **51**, 1344 (1995).
[11] F. Leal Calderon, J. Bibette, and J. Biais, Europhys. Lett. **23**, 653 (1993).
[12] E. J. Meijer and D. Frenkel, J. Chem. Phys. **100**, 6873 (1994).
[13] J. Y. Walz and A. Sharma, J. Colloid Interface Sci. **168**, 485 (1994); see also Y. Mao, M. E. Cates, and H. N. W. Lekkerkerker, Physica A (to be published).
[14] See, for example, Sec. 74 in L. D. Landau and E. M. Lifshitz, *Statistical Physics*, 3rd ed. (Pergamon, Oxford, 1989), Pt. 1.
[15] H. N. W. Lekkerkerker, Colloid Surf. **51**, 419 (1990).
[16] N. F. Carnahan and K. E. Starling, J. Chem. Phys. **53**, 600 (1970).
[17] K. R. Hall, J. Chem. Phys. **57**, 2252 (1972).
[18] H. Reiss, J. Phys. Chem. **96**, 4736 (1992).
[19] S. Erbil, W. C. K. Poon, and P. B. Warren (unpublished).
[20] J. Des Cloizeaux and G. Jannink, *Polymers in Solution* (Oxford University Press, New York, 1990).
[21] G. C. Berry, J. Chem. Phys. **44**, 1550 (1966).
[22] P. N. Pusey, A. D. Pirie, and W. C. K. Poon, Physica A **201**, 322 (1993).
[23] W. C. K. Poon, A. D. Pirie, and P. N. Pusey, Faraday Discuss. (to be published).
[24] R. T. DeHoff, *Thermodynamics in Materials Science* (McGraw Hill, New York, 1993).
[25] H. N. W. Lekkerkerker and A. Stroobants, Physica A **195**, 387 (1993).
[26] W. C. K. Poon and P. B. Warren, Europhys. Lett. **28**, 513 (1994).
[27] A. T. Clark and M. Lal, J. Chem. Soc., Faraday Trans. 2 **77**, 981 (1981).